HST/STIS Spectroscopy and Modeling of the Long Term Cooling of WZ Sagittae following the July 2001 Outburst [1]

Patrick Godon[2] and Edward M. Sion

Department of Astronomy & Astrophysics, Villanova University, Villanova, PA 19085; patrick.godon@villanova.edu emsion@ast.villanova.edu

Fuhua Cheng

Center for Astrophysics, University of Science and Technology of China, Hefei, Anhui 230026, People's Republic of China

Knox S. Long

Space Telescope Science Institute, 3700 San Martin Drive, Baltimore, MD 21218; long@stsci.edu

Boris T. Gänsicke

Department of Physics, University of Warwick, Coventry CV4 7AL, United Kingdom; Boris.Gaensicke@warwick.ac.uk

Paula Szkody

Department of Astronomy, University of Washington, Seattle, WA 98195; szkody@astro.washington.edu

ABSTRACT

We present the latest *Hubble Space Telescope (HST) Space Telescope Imaging Spectrograph (STIS)* E140M spectrum of the dwarf nova WZ Sge, obtained in July 2004, 3 years following the early superoutburst of July 2001. This far-ultraviolet (FUV) spectrum covers the wavelength interval 1150-1725 Å, revealing Stark-broadened Lyα absorption and absorption lines due to metals from a range of ionization states. The Lyα and CIV double peak emissions are still present, indicating the presence of an optically thin disk. Single white dwarf synthetic spectral fits (using $\log g = 8.5$) to the data indicate that the white dwarf has now reached a temperature $T \approx 15,000 \pm 500$K.

Three years after the outburst the WD is still ~1500K above its quiescent temperature, it has an FUV flux level almost twice its pre-outburst value, and its

spectrum does not distinctly exhibit the quasi-molecular hydrogen feature around 1400 Å which was present in the *IUE* and *HST/GHRS* pre-outburst data. This is a clear indication that even three years after outburst the system is still showing the effect of the outburst.

Taking into account previous temperature estimates obtained during the earlier phase of the cooling, we model the cooling curve of WZ Sge, over a period of three years, using a stellar evolution code including accretion and the effects of compressional heating. Assuming that compressional heating alone is the source of the energy released during the cooling phase, we find that (1) the mass of the white dwarf must be quite large ($\approx 1.0 \pm 0.2 M_{\odot}$); and (2) the mass accretion rate must have a time-averaged (over 52 days of outburst) value of the order of $10^{-8} M_{\odot} \mathrm{yr}^{-1}$ or above. The outburst mass accretion rate derived from these compressional heating models is larger than the rates estimated from optical observations (Patterson et al. 2002) and from a FUV spectral fit (Long et al. 2003) by up to one order of magnitude. This implies that during the cooling phase the energy released by the WD is not due to compressional heating alone. We suggest that ongoing accretion during quiescence at a moderately low accretion rate can also release a significant amount of energy in the form of boundary layer irradiation, which can increase the temperature of the star by several thousand degrees.

Subject headings: Cataclysmic variables – stars: individual (WZ Sge) – white dwarfs.

1. Introduction

With an orbital period of 82 minutes, a recurrence time of 33 years, and a visual magnitude "jumping" from 15 to 8 during outburst, the well-studied and widely known system WZ Sge is the prototype of a group of H-rich cataclysmic variables that have the shortest orbital period, longest outburst recurrence time and largest outburst amplitude of any class of dwarf novae (Howell et al. 1999, 2002). With a distance of only $\approx$ 43.4 pc (Thorstensen 2003;

---

[1]Based on observations with the NASA/ESA *Hubble Space Telescope*, obtained at the Space Telescope Science Institute, which is operated by the Association of Universities for Research in Astronomy, Inc., under NASA contract NAS5-26555.

[2]Visiting at the Space Telescope Science Institute, Baltimore, MD 21218, godon@stsci.edu

Harrison et al. 2004) it is also the closest cataclysmic variable, and the brightest dwarf nova. The inclination of the binary is high enough (78 degrees) that the secondary star eclipses the disk rim but not the white dwarf. Recent estimates of the mass of the accreting white dwarf range from $\approx 0.8M_{\odot}$ to $1.2M_{\odot}$ (Spruit & Reuten 1998; Skidmore et al. 2000; Steeghs et al. 2001; Long et al. 2004). Steeghs et al. (2001) found the radial velocity semi-amplitude, K_2, of the secondary star to be in the range 493 km s^{-1} to 585 km s^{-1} giving an upper limit to the mass of the secondary of $M_2 < 0.11M_{\odot}$.

The system went into outburst in 1913, 1946, and 1978 and its recurrence time was therefore assumed to be 33 years. However, on 23 July 2001 the system went into a premature outburst, 10 years earlier than expected. It was first reported by T. Ohshima (see Ishioka et al. (2001)), and was then the object of a multi-wavelength campaign. The July 2001 outburst was the most thoroughly watched dwarf nova eruption in history. The system was in outburst for a total of 52 days (consisting of a primary burst lasting 24 days, followed by a series of echo outbursts) and on the 53rd day of outburst, the active large accretion phase ended and the system started to fade without any other noticeable outburst event (for a complete description of the outburst in the optical see Patterson et al. (2002)).

The outbursts of dwarf novae are believed to be based on a thermal instability of the accretion disk surrounding the WD. During outburst the disk undergoes a transition from a low-temperature neutral state to a high-temperature ionized state. Even though accretion disks appear in many systems of different sizes (ranging from active galactic nuclei to low-mass X-ray binaries), dwarf novae (because of their observability) are still the best laboratories to study the physics of accretion disks. And because of its proximity and intensity, the 2001 July outburst of WZ Sge presented an ideal opportunity to study the outburst mechanism, which prompted extensive observations from optical to X-ray wavelengths.

Far Ultraviolet Spectroscopic Explorer (FUSE) (with a wavelength range of 905-1182 Å) and *HST/STIS* (covering 1150-1730 Å) spectra of the dwarf nova WZ Sge were obtained during and following the early superoutburst of July 2001, over a time span of 2 years (Knigge et al. 2002; Long et al. 2003; Sion et al. 2003; Long et al. 2004). The system evolved during and after the primary outburst and by the end of the rebrightening (echo outbursts) phase the spectrum started to be dominated by the emission of the cooling WD. As the system went into quiescence, the WD temperature was determined accurately. The results showed a cooling in response to the outburst by about 12,000K, from $\approx 28,000$K in 2001 September to $\approx 16,000$K in 2003 March (Long et al. 2003; Sion et al. 2003; Long et al. 2004). In a previous work (Godon et al. 2004) we considered the above FUV observations of WZ Sge during the cooling phase, and, using two different methods, we independently re-derived the temperature of the white dwarf. In this manner we accurately assessed the error bars of the

cooling curve of the white dwarf. In that work, we then modeled the heating and subsequent cooling of the white dwarf using a one-dimensional quasi-static evolution code, and found that the mass of the WD must be large ($\approx 1.2 M_{\odot}$) and it must accrete at a high accretion rate ($9 \times 10^{-9} M_{\odot}\mathrm{yr}^{-1}$) if compressional heating is the only source of energy released by the WD during quiescence. We concluded that ongoing accretion at a low rate during quiescence is needed to explain the observations if the WD has a mass $M = 0.9 M_{\odot}$ and is accreting at a rate $\dot{M} = 3 \times 10^{-9} M_{\odot}\mathrm{yr}^{-1}$ during outburst as inferred by the FUV spectral fits.

A 28-29 s periodic oscillation was also observed both in the optical (Patterson et al. 2002) and in the FUV (Welsh et al. 1997, 2003) as well as a possible harmonic at 15 s during the 2001 outburst (Knigge et al. 2002). Since this oscillation is not always present and does not always have the same period, it is difficult to associate it with the spin of the WD. In addition, if the 29 s signal was indeed caused by the rotation of WD, that would imply a rotational velocity of about 3200km s^{-1} (assuming a 0.9 $M_{\odot}$ WD), much larger than observed. The suggestion that it could be ZZ Ceti-like pulsations of the WD has also been ruled out because the oscillation period did not change significantly while the WD cooled by many thousands of degrees (Welsh et al. 2003). Some of the alternatives left for the origin of this oscillation could be the inner disk, the boundary (or spread) layer or even a fast rotating accretion belt. A time analysis of the July 2004 data will be carried out elsewhere.

In the current work we present and analyze the latest *HST/STIS* spectra obtained in July 2004, namely, 3 years after outburst. This latest observation provides us with an additional data point in the cooling curve to assess the long term cooling of the WD. To be consistent with our previous analysis in Godon et al. (2004), we analyze here the spectrum using exactly the same method. We confirm our previous result that the accreting white dwarf must be fairly massive, as suggested by other types of analyses, and must have been accreting during the super-outburst at a time-averaged mass rate of the order of $\dot{M} \simeq 10^{-8} M_{\odot}\mathrm{yr}^{-1}$. However, our analysis also requires on-going accretion during the cooling phase.

2. The July 2004 *STIS* Spectrum: Observations and Description

The observations took place on 2004, July 11 (starting UT 06:23:35 ; 1083 days post-outburst), with *HST/STIS* using the FUV MAMA detector configuration in TIME-TAG (photon-counting) mode with the medium resolution E140M echelle grating and the 0.2" x 0.2" aperture. In this configuration the wavelength coverage is 1140 - 1735 Å, centered at 1425 Å. The observations consisted of 5 *HST* orbits totaling 13,700s of good exposure time. The primary goal of obtaining 5 consecutive orbits was to determine the mass of the white dwarf (Steeghs et al. 2005). The data reduction was carried out with the standard STScI

pipeline reduction system, namely, using CalSTIS version 2.15c (January 29, 2004). The spectra from the individual spectral orders of the echelle grating were spliced and binned to a resolution of 0.1 Å for our analysis. The results of the line identifications are presented in Figure 1 in which we have co-added the 5 individual spectra obtained from each *HST* orbit.

First, we notice that there is an additional drop in the continuum flux level (measured between 1425 Å and 1525 Å) from $\approx 6\times10^{-14}$ ergs cm^{-2}s^{-1}Å^{-1} in March 2003 to $\approx 4.5\times10^{-14}$ ergs cm^{-2}s^{-1}Å^{-1} in July 2004 (see Table 1 where we recapitulate the *STIS* observations starting 2001 September 11), suggesting that the white dwarf keeps on cooling. The 2004 July flux level is still 1.8 times larger than the pre-outburst flux level recorded in late quiescence by *IUE* (10-14 years since outburst) and *HST/GHRS* (17 years since outburst). In Table 2 we list some quiescent *IUE* spectra of WZ Sge, the average flux level (also measured between 1425 Å and 1525 Å) is $\approx 2.6 \times 10^{-14}$ ergs cm^{-2}s^{-1}Å^{-1}. In Figure 2 we draw the 2004 July 11 *HST/STIS* spectrum together with the 1989 August 26 *IUE* spectra (SWP36885) for comparison. Both from Table 2 and Figure 2 it is obvious that WZ Sge has not yet reached its deep quiescence flux level.

The spectral coverage of *STIS* for the E140M echelle grating setup is fixed (1140 Å - 1725 Å , though the region between 1140 Å and 1150 Å is usually too noisy and is being dropped). Consequently all the *STIS* spectra of WZ Sge considered in the present work have all the same spectral coverage. This makes the suite of *STIS* observations of WZ Sge all directly comparable. Therefore, in Table 1 we also list the flux integrated ($\int d\lambda$) over the entire spectral range of STIS, to the power 1/4, for all the epochs, which is proportional to the effective temperature. In the last column of the Table we list the temperatures derived in Long et al. (2004) and the ones re-estimated by Godon et al. (2004) together with the present results (presented in Table 4, see next section).

The most prominent line feature in the spectrum is the very broad Lyα absorption which we attribute to the high-gravity white dwarf photosphere. One does not see distinclty the H_2 quasi-molecular absorption feature (centered around 1400Å) in the spectrum, which was observed and modeled during deep quiescence in the *HST/FOS* spectra of the system (Sion et al. 1995). This feature is expected to emerge now as the WD temperature is well below 20,000K. The spectral signature of the Hydrogen quasi-molecular absorption is a pronounced drop in flux just shortward of ≈1400 Å, as can be clearly seen in the *IUE* spectrum in Figure 2.

Other prominent features in the spectrum are the broad emission wings at C IV (1548 Å, 1550 Å, flanking deep absorption) and the double-peaked Lyα feature in emission. They both might be associated, at least in part, with the system and are generally assumed to arise from the disk. A close examination of the individual exposures reveals that the double-peaked

features have the blue emission peak higher than the red peak (this is much more pronounced in the C IV than in the Lyα). A rough measurement of the peak-to-peak separation gives 5Å. At Lyα, 1Å corresponds to about 245 km s^{-1} (and the 0.1 Å resolution corresponds to 25 km s^{-1}), so that this separation corresponds to roughly 1225 ± 25 km/s. This leads to a value of the disk velocity $V_{disk} \times \sin i = 613$ km s^{-1}. For comparison, Skidmore et al. (2000) measure $V_{disk} \times \sin i = 723$ km s^{-1} from the Balmer Hα for WZ Sge in quiescence. These values for Lyα suggest a disk-formed line, and are consistent with the work of Mason et al. (2000) who report several disk velocities. The Lyα and CIV double peak emissions indicate the presence of an optically thin disk. This optically thin disk could contribute to the continuum, however, the flux in the core of the Ly alpha line drops close to zero, therefore limiting the amount of optically thin emission (or any other thermal low gravity emission).

The other features are predominantly absorption lines covering a broad range of ionization. Of immediate interest is the mix of ions, the excitation/ionization states of the transitions and the differences one sees between this spectrum and the spectra of WZ Sge obtained previously, e.g. Figures 1-4 (for the September, October, November and December 2001 spectra respectively) in Sion et al. (2003) and Figures 3, 2 & 4 (for the April 2002, August 2002 and March 2003 spectra respectively) in Long et al. (2004). See also Figure 1 in Long et al. (2003) for a direct comparison of the flux level of the *HST/STIS* spectra between September 2001 and March 2003. Carbon and Silicon absorption lines are observed for a whole range of ionization levels: C I, C II, C III, C IV, Si II, Si III, and Si IV. We also observed Al II, Fe II, O I, N I and N V. And we tentatively identify S I, S II, S III, Al I, N II , N III and possibly also Ni II, Cu II, and Co II. Many of these absorption lines are due to material local to WZ Sge, since the close distance of WZ Sge (43pc) precludes an ISM origin. We recapitulate all the lines we identified in Table 3. For each line we list the line center, the line width, the line shift and in the last column we specify whether these measurments were carried out for the combined data (summed over the 5 orbits) or for an individual orbit.

We note that to produce substantial Si IV absorption lines in the WD photosphere requires temperatures above about 25,000K, basically 10,000K larger than the WD present temperature. This suggests that the Si IV lines do not originate in the WD photosphere. The same is true for N V which requires a much higher temperature ($T \sim 80,000$K) than Si IV. It is noteworthy here that N V is seen in absorption in the dwarf nova U Gem during quiescence but does not share the same velocity as the gravitationally-redshifted white dwarf photosphere (Sion et al. 1998; Long & Gilliland 1999). This feature is thought to arise in an extended hot region of gas near the white dwarf in U Gem.

We note that the following strong absorption lines were not (or only weakly) seen in

the 2003 March *HST/STIS* spectrum: C I 1277.3, 1277.5 Å, C I 1328.8-1329.6 Å, and N I 1492.63, 1492.82, 1494.68 Å, while N V has become less prominent. In the present spectrum the width of all the broad absorption lines varies slightly from (HST) orbit to orbit (by up to 0.5 Å) and is similar to the width observed in the 2003 March spectrum (Long et al. 2004). Therefore, within this 0.5 Å accuracy the width of the lines is similar to the width measured in March 2003 by Long et al. (2004).

There are also unidentified features between 1430Å and 1440Å which we tentatively identify as a blend of mainly C I with probably Si I and possibly Al I. Such features were seen in the quiescence spectra of WZ Sge (Sion et al. 1995; Cheng et al. 1997). The C II 1335Å ionization lines do not resemble expected photospheric features as they are too deep (see also the results in next section).

In order to differentiate between the lines that are associated with the white dwarf (i.e. with the same velocity and/or broadening) and the lines that are not associated with it (i.e. associated with the binary but in a shell or external ring), we check how the profile of a given absorption line changes from one (spacecraft) orbit to another. The line widths and wavelengths were measured and checked by a careful inspection of the spectrum. We find that the following absorption lines have the same width and the same wavelength during the entire observations: C I 1266.42 Å, Al I 1271.77 Å, C I 1277.3, 1277.5 Å, O I 1302.17 Å, N I 1316.04 Å, Cu II 1442.14 Å, Co II 1443.84 Å, and Co II 1456.27 Å. These are very sharp absorption lines and are obviously not associated with the WD nor with its companion as they do not exhibit any velocity change: within the accuracy of our binning of 0.1 Å all these lines are at the expected laboratory wavelength. Because of the proximity of WZ Sge we identify these lines with the system albeit outside the binary itself. On the other hand, the broader and deeper absorption lines exhibit a wavelength shift of about 0.3-0.5 Å from (spacecraft) orbit to orbit, corresponding to a velocity of up to 120km s^{-1}, where in the first orbit the line appears to be blue-shifted and in a later orbit (usually the 4th) the line appears to be at its laboratory wavelength. However, for the N V doublet lines, it seems to be the opposite: in the first orbit the lines are at the rest frame velocity and in the later orbits the line are red-shifted by 0.4 Å. This is more clearly observed for the N V 1242.80 Å line than for the N V 1238.82 Å line, as the N IV doublet lines are not very strong and the flux level at this wavelength is rather low. If correct, this points to the fact that the N V lines might form in a region which has a velocity of $\approx$ 100 km s^{-1} (away from the observer) relatively to the velocity of the WD, similar to what is observed for U Gem. The N V lines in U Gem have velocities which are different from the other lines both in outburst and quiescence (Sion et al. 1998; Long & Gilliland 1999).

A detailed study of the radial velocities (RV study) of the absorption lines together with

a K1 determination is being carried out elsewhere (Steeghs et al. 2005).

2.1. The Synthetic Spectral Modeling of the July 2004 Spectrum of WZ Sge

In order to determine the parameters of the white dwarf from the *HST/STIS* spectrum, we compare the observed spectrum with a grid of theoretical synthetic spectra generated with Ivan Hubeny's model atmosphere and spectrum synthesis codes TLUSTY200 and SYNSPEC48 (Hubeny 1988; Hubeny et al. 1994; Hubeny & Lanz 1995). We take the white dwarf photospheric temperature T_{eff}, its gravity $\log g$, its photospheric chemical abundances, and its rotational velocity $V_{rot} \sin i$ as free parameters. The comparison is then carried out using a χ^2_ν minimization fitting procedure (Press et al. 1992). More details about the minimization technique, including the scaling parameter, can also be found in Sion et al. (2003).

In preparation for the fitting of the models we mask these regions of the spectrum which exhibit spectral features not originating in the WD photosphere and which can signficantly affect the fitting: the N V doublet in absorption around 1240 Å; the Si IV doublet in absorption around 1400 Å; and both the Lyα (around 1215 Å) and CIV (around 1550 Å) double peak emissions. It is important to note that the N V region overlaps the longward wing of the Lyα absorption profile, which is very sensitive to the temperature. The sharp absorption lines which are most probably not associated with the WD are not masked, as they are so sharp that they do not affect the fitting at all. In addition some of these sharp absorption lines are on top of broader absorption lines/features which themselves could be due to the WD.

We use three slightly different approaches in parallel to assess quantitatively the uncertainty in the spectral fitting technique. Following the nomenclature we adopted in Godon et al. (2004) we denote the three different methods by (a), (b) and (c), where (c) is really the method used by Long et al. (2004) while (a) and (b) were used in Godon et al. (2004).

In (a) each individual spectrum (for each spacecraft orbit) is fit to a synthetic stellar atmosphere spectrum, Si and C abundances are fitted separately and the regions that are masked are: 1209-1223 Å, 1236-1246 Å, 1380-1410 Å and 1538-1560 Å. In (b) and (c) the spectral fit is carried out on the co-added spectra (from the 5 orbits) and scaled solar abundances are used. In (c) the masked regions are: 1206-1226 Å, 1233-1246 Å, 1390-1410 Å and 1538-1560 Å. In (a), however, only the region around the Ly alpha core is cut out but Gaussian emission components are included for N V, C IV and He II (1640 Å). Method (a) and (b) assumed $\log g$ = 8.5, while in method (c) three different values of $\log g$ were assumed: 8.0, 8.5 and 9.0.

2.2. Determination of the WD Parameters

The best-fitting white dwarf models to the July 2004 observations are displayed in Table 4. These best-fit results all give fairly reasonable χ^2_ν values and, as a result of this, one cannot use the spectral fits alone to select the gravity of the WD. Instead, one has to use the fact that in the fitting methods, the radius of the white dwarf is part of the results when scaling the flux to the distance to the source (43.4 pc). The radius obtained (as output in Table 4) for the $log(g) = 8.5$ models is consistent with the radius inferred from the $log(g) = 8.5$ assumption (e.g. see the mass radius relation from Hamada & Salpeter (1961) or see Wood (1990) for different composition and non-zero temperatures WDs). This is not the case for the $log(g) = 8.0$ and $log(g) = 9.0$ models, in which the radius is not self-consistent with the $log(g)$ assumption.

We therefore adopt the $log(g) = 8.5$ solution as the best fit, for which we find that the WD has a temperature of $15,000\text{K}\pm 500\text{K}$ (this is the average temperature of the best fits in Table 3), a radius of $6.2 \pm 0.4 \times 10^8$cm, a rotational velocity between 250 and 700km s^{-1} and non-solar abundances.

For log$(g) = 9.0$ (a $1.2M_\odot$ white dwarf) the best fit models lead to temperatures about 1000K larger, while for $log(g) = 8.0$ ($0.6M_\odot$) the the temperatures are cooler by about the same amount (≈1000K). The rotational velocities and composition, however, do not change significantly as a function of $log(g)$.

As in Godon et al. (2004) we also compute the “flux-based” temperature. For this purpose we take the 4th root of the integrated flux listed in Table 1, and scale the value obtained with the same factor as in Godon et al. (2004), such that for the March 2003 data, the flux-based temperature fits the temperature assessed using method (b). The flux-base temperatures fall all within the average values estimated by method (a), (b) and (c) for the entire 3 year period of observations. The flux level in the first orbit of July 2004 was slightly larger than in orbits 2-5, and this translates as an increase in temperature of about 400K.

In Figure 3 we display the $\log g = 8.5$ best fit model using method (c), in Figure 4 we display the best fit model using method (b), and in Figure 5 we display the best fit model to orbit 2 using method (a). All the other best-fit models listed in Table 4 are similar to the results we show in Figures 3, 4, 5. In these Figures we note that the 4 regions we masked (in green in Figure 3) are, as expected, in significant disagreement with the observations. Another region where the models do not fit the observed spectrum is in the range $\lambda \approx 1330 - 1365$ Å, where the observed C II $\simeq 1335$ Å and C I (+ O I + Si II) $\simeq 1355$ Å are much deeper than in the models. It is not clear whether the observed excess (in comparison to the models) of flux around 1340 Å is a “wing” that belongs to the C I

line or to the C II line. In model (b) this feature has been fitted with a Gaussian emitting component. At short wavelengths there seems to be a systematic excess emission (especially noticeable on both sides of the double peak Lyα emission). This is probably due to the decline in the effective area of *STIS* at short wavelengths. Calibration files that correct for this problem do not currently exist for the echelle grating modes. This excess emission could also be due to the presence of a second component, possibly an optically thin quiescent accretion disk (see section 3.2).

The rotational velocity, $V_{rot} \sin i$ is of the order of 250 km s^{-1} (as derived by method c) and could be as high as 700 km s^{-1} (as derived by method a), depending on the metallicity one uses in the models. This is about the same value as observed in 2003 March and before. This velocity, if it corresponds to the true underlying white dwarf is far lower than the value of 1200 km s^{-1} found by fitting the GHRS data (Cheng et al. 1997) during deep quiescence. Long et al. (2004) re-examined the GHRS data and found an even higher velocity $V_{rot} \sin i \approx$2000 km s^{-1}, but they also noted that there is a correlation between rotational velocity and metallicity, and that the implied metallicity was also very high. As the metallicity increases in the models, the rotational velocity also must increase in order to match the depth of the lines. Initially the *STIS* observations from to 2001 to March 2003 revealed that the rotational velocity was increasing with time reaching a maximum in March 2003 (Long et al. 2004). It was therefore expected that as the WD was evolving deeper into quiescence its rotation rate would eventually match the one observed before outburst with GHRS. The understanding was that with time the WD was revealing its stellar surface and that by 2004 we would be able to observe the rotation of the WD with no or little contamination from line-of-sight absorption. But the 2004 July observation seems to indicate a lower rotation rate.

3. The Heating and Long-Term Cooling of the White Dwarf

In Table 1 we listed the WD temperature range for the 10 *HST/STIS* observations that were obtained over a period of 3 years following the 2001 July outburst (Sion et al. 2003; Long et al. 2004). Long et al. (2003) also estimated the temperature from two *FUSE* observations. The *HST/STIS* derived temperatures were independently re-assessed in Godon et al. (2004) using method (a) and (b) and the integrated flux as described in the previous section. These different methods were considered in Godon et al. (2004) and here in order to explicitly assess the error in the temperature. In Figure 6 we plot the observed cooling curve (with symbols as marked in the graph) of the WD as it appears from these observations (including the two early data points obtained with *FUSE*, (Long et al. 2003)). The main difference with the observed cooling curve from Godon et al. (2004) is the addition of the last data point,

the 2004 July *HST/STIS* data. Before we proceed to the description of the modeling of the heating and cooling of the WD, it is important to note that the temperatures listed in Table 1 and displayed in Figure 6 were all obtained assuming $\log(g) = 8.5$, which corresponds to a $0.9M_{\odot}$ white dwarf mass. We recall here that for $\log(g) = 9.0$ the entire cooling curve shifts upward by about 1000K, and similarly for $log(g) = 8.0$ the curve shifts downward by about 1000K.

In order to model the accretional heating and subsequent cooling of the WD in WZ Sge, we used a 1D evolutionary code without hydrodynamics (quasi-static assumption). It is an updated version of the quasi-static stellar evolution code of Sion (1995) and more details can be found there. We carried out numerical simulations by switching on accretion for the duration of the superoutburst and then shutting it off to follow the cooling of the white dwarf. In this way the effects of compressional heating can be assessed quantitatively. The matter was assumed to accrete 'softly' with the same entropy as the white dwarf outer layers. It was also assumed that the accretion and heating of the white dwarf was uniform rather than being restricted to the equatorial region. The transfer of angular momentum (by shear mixing) into the white dwarf was neglected.

During the actual outburst, as accretion took place at a high rate, the star's photospheric emission was overwhelmed by the emission of the hot components (mainly the inner disk), which made it difficult to assess the exact temperature of the star and its rotation rate Ω_{wd}. However, on day 53 the large accretion phase ended. By that time the accretion rate had probably dropped to its quiescence level. Therefore, we modeled the superoutburst of WZ Sge by turning on the accretion (at a constant rate) for 52 days, after which it was shut off and the model was evolved for $\sim$3 years (1200 days). The exact outburst mass accretion rate of the system is not known, however, it seems very likely that initially the mass accretion rate was very high at the onset of the outburst and decreased steadily during the plateau phase and then it was more erratic during the "echo outbursts " phase resembling a succession of normal dwarf nova outbursts. It has been shown (Godon & Sion 2002) that compressional heating is primarily a function of the accreted mass and that the time dependence of the mass accretion rate has little effect on the compressional heating after that mass has been accreted. This justifies the use of a constant mass accretion rate in our simulations. In addition, at the present time our code cannot simulate a variable mass accretion event ($\dot{M} \neq constant$).

3.1. Compressional Heating and Subsequent Cooling

In the first set of simulations we assume that the observed elevated temperature of the star is due to the compressional heating it has endured during the outburst phase *alone*, and

this energy is released slowly during the cooling phase. Namely, we neglect the boundary layer irradiation during outburst, as it was shown (Godon & Sion 2002) that the temperature increase due to BL irradiation is sustained only during accretion, and when the accretion is turned off, the star rapidly radiates away the BL energy absorbed in its outermost layer. However, the temperature increase due to compressional heating takes place deeper in the layers of the star and it takes many days (years) for the star to cool.

We ran models with different white dwarf mass, namely $M_{wd} = 0.8M_{\odot}$ to $1.2M_{\odot}$ (by increments of $0.1M_{\odot}$) and varied the mass accretion rate in the range $10^{-9}M_{\odot}\mathrm{yr}^{-1}$ – $10^{-8}M_{\odot}\mathrm{yr}^{-1}$ (by increments of about 10% of its value). We chose the initial WD temperature ranging from 12,000-15,000K by increment of 500K. We take into account the $log(g)/T_{wd}$ degeneracy of the models as stated at the beginning of this section, namely, the observed cooling curve displayed in Figure 6 shifts upward by 1000K when considering the $log(g) = 9.0$ solutions and shifts downward by 1000K when considering the $log(g) = 8.0$ solutions. For each different WD mass (models 1, 2, 3, 4, & 5 in Table 5) we find a mass accretion rate that accounts for the elevated temperature of the white dwarf with a corresponding simulated cooling curve fitting the data points. However, as mentioned previously, the synthetic spectral fit in this work and in Long et al. (2004) are all consistent with a $M = 0.9M_{\odot}$ accreting white dwarf. This is the reason why we display in Figure 6 the best fit model for a $0.9M_{\odot}$ WD (model 2 in Table 5) accreting at a rate of $2.8 \times 10^{-8}M_{\odot}\mathrm{yr}^{-1}$. All the other best fits listed in Table 5 (with a different WD mass) fitted the observed cooling curve as well (except model 6, which we consider in the next subsection). From these simulations, the quiescence WD temperature is $\approx 13,500 \pm 1000$K, and the average mass accretion rate of the outburst models (a few $10^{-8}M_{\odot}\mathrm{yr}^{-1}$) is larger by about one order of magnitude than the value determined from the spectral fits to the observations during the outburst phase ($\approx 3 \times 10^{-9}M_{\odot}\mathrm{yr}^{-1}$ (Long et al. 2003)). It could be that during the outburst the disk actually is self-absorbing/self-occulting and therefore the mass accretion rate derived from the observations during outburst might have been under estimated.

In the last column of the table we also list the numerically computed excess energy that is radiated by the WD during and following the outburst over 1200 days. We see that it is around $2 - 3 \times 10^{39}$ergs and it increases to $7 - 8 \times 10^{39}$ergs when we integrate the numerical models over a period of 10,000 days (27.4yrs). The computed excess energy radiated by the WD here is only a few percent of the corresponding theoretical accretion energy derived from the mass accretion rate given in Table 5. This is similar to Gänsicke & Beuermann (1996) who obtained a value of only 1 percent for VW Hyi. For comparison, the total outburst energy derived in Patterson et al. (2002) (which is partially based on the FUV data) is 4.6×10^{40}ergs over the 24 days main outburst (20 percent more is radiated over the next 100 days) and is also about 10 times less than the accretion energy assumed

in the compressional heating simulations. This is the same discrepancy that was mentioned before in the mass accretion rate and it arises because the accretion rate needed to reproduce the cooling curve is more than one order of magnitude larger than derived from the spectral fits during outburst (Long et al. 2003). In other words, the accreted mass derived from the observations, $\Delta M = 4 \times 10^{23}$g(d/43pc)$^2(M_{wd}/M_\odot)^{-1.8}$ (Patterson et al. 2002), is one order of magnitude smaller than the accreted mass needed in the compressional heating simulations (5.7×10^{24}g) to reproduce the observed cooling curve. Due to the extreme mass ratio, the difference compared to the compressional heating simulations could even be larger.

This discrepancy can be accounted for if during the cooling phase the WD actually releases energy that does not originate from the compressional heating. This energy could include rotational kinetic energy released from the outer layer of the star which was spun up during the outburst phase (Kippenhahn & Thomas 1978; Sparks et al. 1993; Long et al. 1993) and/or ongoing accretion after the outburst (Long et al. 1993; Godon et al. 2004). Since it is not known how much rotational kinetic energy might be stored in the outer layer of the star and currently no model exists to assess this energy (such a model would require two-dimensional simulation of the accretion including a treatment for the outer envelope of the star), we consider here only ongoing accretion after outburst as a source of additional energy release during the cooling phase (see next subsection).

3.2. Boundary Layer Irradiation During Quiescence

We compute here a $0.9M_\odot$ model (model 6 in table 5) with a mass accretion rate of $\dot{M} = 5 \times 10^{-9} M_\odot \mathrm{yr}^{-1}$, of the same order (though slighlty larger) than the mass accretion rate inferred from the *FUSE* observations on day 7 of the outburst phase $\dot{M} = 1 - 3 \times 10^{-9} M_\odot \mathrm{yr}^{-1}$ Long et al. (2003). We display this model in Figure 7, from which it is clear that compressional heating alone cannot account for the observed cooling curve : its temperature is too low by ≈1,000K in July 2004 and $6 - 7,000$K in Fall 2001.

We suggest here that on-going accretion during quiescence can increase the temperature of this model to match the observed cooling curve. As was shown in Godon et al. (2004), during low quiescent accretion, boundary layer irradiation can substantially increase the temperature of the WD. However, in order to be consistent with the observations, this accretion rate must be lower than the limit inferred from the FUV observations. The strictest limit on this emission is near 1216 Å, where very little flux is expected from the WD, and the observed flux level was 5×10^{-15}ergs cm^{-1}s^{-1}Å^{-1}. To assess the maximum accretion rate allowed, we consider the simulated disk spectra produced by Wade & Hubeny (1998). For or a $0.8M_\odot$ WD with a mass accretion rate of $3 \times 10^{-11} M_\odot \mathrm{yr}^{-1}$ and an inclination of

78 degrees, the Wade and Hubeny simulations suggest a flux of 1.6×10^{-14}erg cm^{-1}s^{-1}Å^{-1} at 43 pc. Thus, a reasonable upper limit to the mass accretion rate in July 2004 was $\simeq 10^{-11} M_{\odot}$yr^{-1}. For the earlier spectra the upper limit to the mass accretion rate increases roughly in the same relative proportion to the continuum flux level near Lyα (see Figure 1 in Long et al. (2004)). As a result, the mass accretion rate then could have been as large as $\approx 5 \times 10^{-11} M_{\odot}$yr^{-1} in 2001 September.

To check this hypothesis of ongoing accretion during the cooling phase, we carry out simulations of boundary layer irradiation for model 6 (Figure 7) during the cooling phase, assuming a temperature 14-16,000K and an accretion rate $\dot{M} = 10^{-11} - 10^{-10} M_{\odot}$yr^{-1}. We list the results in Table 6. The initial WD temperature T^i_{wd} listed in column 5 represents the temperature of the WD of model 6 in Figure 7 (solid line) around $t \sim 500 - 1000$ days (14,000K) and around $t \sim 100$ days (16,000K). A temperature increase of 1,000K to 4,000K is obtained for a quiescent mass accretion rate for models 6 through 11. However, one would need an accretion of $\approx 10^{-10} M_{\odot}$yr^{-1} in order to increase the temperature by 6,400K (model 12), to match the discrepancy of model 9 around day 100. We therefore suggest that the real picture is probably somewhere between model 9 (with accretion during the cooling phase) and model 2 (where all the heating is due to compressional heating). Spectral fits to the earlier *HST* data (Sion et al. 2003; Long et al. 2004) were in better agreement (in a χ^2_{ν} speaking sense) with stellar spectra alone than with combined disk-stellar spectra, however the combined disk-stellar spectra could not be ruled out unambiguously. One of the problems we are facing here is that at such low accretion rates the quiescent disk is probably optically thin and accurate spectral models of its continuum do not exist.

4. Conclusion

Our main purpose in analyzing the 2004 July spectrum of WZ Sge was to determine the temperature, mass, rotation rate and chemical abundances of the accreting white dwarf in the system. The temperature was needed to assess the cooling of the WD 3 years after the outburst, and we found that the WD's temperature is still higher than it was before outburst. We confirmed that the mass of the WD is large and we inferred from the spectral fit a value of $0.9 M_{\odot}$ in agreement with Long et al. (2004) and Steeghs et al. (2005). However simulations of post-outburst cooling due to the effects of of compressional heating of a $0.9 M_{\odot}$ WD as well as ongoing quiescent accretion fit the observed cooling only if the mass accretion rate is larger than observed. Compressional heating simulations with a mass accretion rate as low as the one inferred from the observations during outburst have a temperature too low by several thousand degrees and one needs to assume on-going accretion during the cooling

phase in order to reduce the temperature discrepancy.

From the spectral fit of the lines we also estimated the chemical abundances and the rotation velocity of the WD. We expected to find a high stellar rotation rate for the WD (1200km s^{-1}, Cheng et al. (1997)) but we found a rotation rate of only a few 100km s^{-1}. However, whether the lines belong to the WD or to material in the line of sight is unclear. Long et al. (2004) have shown that slab models can fit the data better and have suggested caution when deriving results obtained from the analysis of the absorption lines, as one cannot distinguish which lines in WZ Sge originate in the WD photosphere and which ones are due to circumstellar or interstellar absorption. What is now needed is self-consistent modeling of the time-resolved spectra, which attempts to disentangle the photospheric lines from those in overlying material. Until such an analysis is successfully completed, it will not be possible to conclusively state the rotation velocity of the WD in WZ Sge.

The N V doublet absorption lines in WZ Sge originates from matter that does not share the same velocity shift as all the other lines (as in U Gem) . We also know for sure that the C IV and Si IV lines are not from the WD, but they are from the system, and it is also quite clear that the sharp absorption lines from Al I, C I, O I, Cu I, Co I, and even N I may not be associated with the white dwarf or cool companion. It is not certain, however, that the remaining absorption lines (which are pretty broad) in the spectrum are from the WD, as their width slightly changes from orbit to orbit (see section 2). This change might be explained if the WD is observed through absorbing material that is located asymmetrically above the disk (the asymmetry could be due to the tidal force of the companion or to matter overshooting the hot spot). From the spectral fit (method a) we find that the chemical abundance Si and C both continue to decrease from 0.4 and 3.5 (respectively) in 2003 March to 0.2 and 2.0 in 2004 July. However, we cannot unambiguously answer the question whether the apparent over-abundance of C relative to Si reflects the actual situation in the photosphere of the white dwarf of WZ Sge.

The flux-based temperature method gives a temperature of about 13,500K for the 1989 IUE spectra (Slevinsky et al. 1999) obtained 11 years after the 1978 outburst which had a flux level 30-50 percent lower than in the July 2004 STIS spectrum, obtained 3 years after the 2001 outburst. This temperature is also the quiescent temperature found in the earlier IUE data (Szkody & Sion 1989; Sion & Szkody 1990). It seems that three years after outburst the WD is still $\simeq$1500K above its quiescent temperature, it has an FUV flux level almost twice its pre-outburst value, and its spectrum does not distinctly exhibit the quasi-molecular hydrogen feature around 1400 Å which was present in the *IUE* and *HST/GHRS* pre-outburst data. This is a clear indication that even three years after outburst the WD in WZ Sge has not yet returned to its deep quiescent state.

We would like to thank the anonymous referee for her/his constructive criticism and prompt report. PG is thankfull to the Space Telescope Science Institute for its kind hospitality.

REFERENCES

Cheng, F., Sion, E.M., Szkody, P., & Huang, M. 1997, ApJ, 484, L149

Gänsicke, B.T., & Beuermann 1996, A&A, 309, L47

Godon, P., & Sion, E. M. 2002, ApJ, 566, 1084

Godon, P., Sion, E.M., Cheng, F., Gänsicke, B.T., Howell, S., Knigge, C., Sparks, W.M., & Starrfield, S., 2004, ApJ, 602, 336

Hamada, T., & Salpeter, E.E. 1961, ApJ, 134, 683

Hasenkopf, C.A, & Eracleous, M., 2002, AAS Meeting 201, 120.03

Harrison, T.E., Johnson, J.J., McArthur, B.E., Benedict, G.F., Szkody, P., Howell, S.B., & Gelino, D.M. 2004, AJ, 127, 460

Howell, S.B., Ciardi, D., Szkody, P., van Paradijs, J., Kuulkers, E., Cash, J., Sirk, M., & Long, K.S. 1999, PASP, 111, 342

Howell, S.B., Fried, R., Szkody, P., Sirk, M., & Schmidt, G. 2002, PASP, 114, 748

Hubeny, I. 1988, Comput. Phys. Comm., 52, 103

Hubeny, I., Lanz, T., & Jeffrey, S. 1994, Newsletter on Analysis of Astronomical Spectra (St. Andrews Univ.), 20, 30

Hubeny, I., & Lanz, T. 1995, ApJ, 439, 875

Ishioka, R. et al. 2001, IAU Circ., 7669, 1

Knigge, C., Hynes, R.I., Steeghs, D., Long, K.S., Araujo-Betancor, S., & Marsh, T.R., 2002, ApJ, 580, L151

Knigge, C., Long, K.S., Hoard, D., Szkody, P., Dhillon, V. 2000, ApJ, 539, L49

Kippenhahn, R., & Thomas, H.-C. 1978, A&A, 63, 265

Kuulkers, E., Knigge, C., Steeghs, D., Wheatley, P.J., Long, K.S. 2002, in "The Physics of Cataclysmic Variables and Related Objects", eds. B.T. Gänsicke, K. Beuermann, and K. Reinsch, ASP Conf.Ser., 261, 443.

Long, K.S., & Gilliland, R.L. 1999, ApJ, 511, 916L

Long, K.S., Blair, W.P., Bowers, C.W., Davidsen, A.F., Kriss, G.A., Sion, E.M., & Hubeny, I. 1993, ApJ, 405, 327

Long, K.S., Froning, C.S., Gänsicke, B., Knigge, C., Sion, E.M., & Szkody, P. 2003, ApJ, 591, 1172

Long, K.S., Sion, E.M., Huang, M., & Szkody, P. 1994, ApJ, 424, L49

Long, K.S., Sion, E.M., Gänsicke, B.T., & Szkody, P., 2004, ApJ, 602, 948

Mason, E., Skidmore, W., Howell, S.B., Ciardi, D.R., Littlefair, S., Dhillon, V.S. 2000, MNRAS, 318, 440

Patterson J., et al. 2002, PASP, 114, 721

Popham, R. 1999, MNRAS, 308, 979

Press, W.H., Teukolsky, S.A., Vetterling, W.T., Flannery, B.P., Numerical Recipes in Fortran 77, The Art of Scientific Computing, Second Edition, 1992, Cambridge University Press.

Regev, O., & Shara, M. M. 1989, ApJ, 340, 1006

Shaviv, G., & Starrfield, S. 1987, ApJ, 321, L51

Sion, E. M. 1995, ApJ, 438, 876

Sion, E.M., Cheng, F.H., Long, K.S., Szkody, P., Gilliland, R.L., Huang, M., Hubeny, I. 1995, ApJ, 439, 957

Sion, E.M., Cheng., F., Szkody, P., Sparks, W.M., Gänsicke, B.T., Huang, M., Mattei, J. 1998, ApJ, 496, 449

Sion, E.M., Gänsicke, B.T., Long, K.S., Szkody, P., Cheng, F., Howell, S.B., Godon, P., Knigge, C., Marsh, T., Sparks, W.M., & Starrfield, S., 2003, ApJ, 592, 1137

Sion, E.M., & Szkody, P. 1990, Proc. IAU Coll. 122, "Physics of Classical Novae", A. Cassatella & R. Viotti (Eds), p.59, Springer-Verlag

Skidmore, W., Mason, E., Howell, S.B., Ciardi, D.R., Littlefair, S., & Dhillon, V.S. 2000, MNRAS, 318, 429

Slevinsky, R.J., Stys, D., West, S., Sion, E.M., & Cheng, R.H. 1999, PASP, 111, 1292

Sparks, W.M., Sion, E.M., Starrfield, S., Austin, S. 1993, in The Physics of Cataclysmic Variables and Related Objects (eds. Regev and Shaviv)

Spruit, H.C., & Reuten, R.G.M. 1998, MNRAS, 299, 768

Steeghs, D., Marsh, T., Knigge, C., Maxted, P.F.L., Kuulkers, E., & Skidmore, W. 2001, ApJ, 562, L145

Steeghs, D., Howell, S.B., Knigge, C., Gänsicke, B.T., Sion, E.M. , 2005, in preparation

Szkody, P., & Sion, E.M. 1989, Proc. IAU Coll. 114, "White Dwarfs", G. Wegner (Ed.), p.92, Springer-Verlag

Thorstensen, J.R. 2003, AJ, 126, 3017

Wade, R., & Hubeny, I. 1998, ApJ, 509, 350

Welsh, W.F., Sion, E.M., Godon, P., Gänsicke, B.T., Knigge, C., Long, K.S., & Szkody, P. 2003, ApJ, 599, 509

Welsh, W.F., Skidmore, W., Wood, J., Cheng, F., & Sion, E.M. 1997, MNRAS, 291, 57

Wood, M.A. 1990, Ph.D. thesis, University of Texas at Austin

This preprint was prepared with the AAS LaTeX macros v5.2.

Table 1. STIS Observation Log with Temperature estimates

Date	Day into Outburst	Exposure (s)	1425-1525 Å Flux (ergs $cm^{-2}s^{-1}Å^{-1}$)	(Integrated Flux)$^{1/4}$ (10^{-3})	T$^{(1)}$ (1000 K)
2001 Sep 11	50	2330	3.9×10^{-13}	3.8	31.9-27.0-28.2
2001 Oct 10	79	2330	2.7×10^{-13}	3.3	25.2-23.6-23.4
2001 Nov 10	110	2330	2.1×10^{-13}	3.1	23.7-22.4-22.1
2001 Dec 11	141	2330	1.7×10^{-13}	2.9	22.6-21.6-20.7
2002 Apr 15	266	5150	1.0×10^{-13}	2.5	19.5-18.8-18.1
2002 Jun 05	317	5150	9.1×10^{-14}	2.5	18.8-18.0-17.4
2002 Aug 27	400	5150	8.0×10^{-14}	2.4	17.8-17.4-16.7
2002 Nov 01	466	5150	6.6×10^{-14}	2.3	17.5-17.0-16.3
2003 Mar 23	608	5150	6.0×10^{-14}	2.2	17.2-16.6-15.9
2004 Jul 11	1083	13700	4.5×10^{-14}	2.0	14.6-15.5-15.4

$^{(1)}$The temperatures were estimated using three different fitting techniques: (a), (b) and (c) respectively. Methods (a) and (b) were used in Godon et al. (2004), while method (c) is from Long et al. (2004) (see section 2.1 for details). The 2004 July temperature is from this work (see Table 4). All these temperatures were estimated assuming $\log g = 8.5$.

Table 2. IUE Observation Log of WZ Sge in deep quiescence

Spectrum	Date	Exposure (s)	1425-1525 Å Flux (ergs $cm^{-2}s^{-1}Å^{-1}$)	Time since outburst (yrs)
SWP33419	1988 May 01	10,800	2.27×10^{-14}	10
SWP36885	1989 Aug 26	10,800	2.79×10^{-14}	11
SWP45103	1992 Jul 08	16,500	2.73×10^{-14}	14
SWP45298	1992 Aug 06	15,600	2.45×10^{-14}	14
SWP45370	1992 Aug 18	11,760	2.59×10^{-14}	14

Table 3. Line Identifications and Absorption Line Measurement, July 2004 Spectrum

Line Identification	Line Center (Å)	Line Width (Å)	Line Shift (Å)	Orbit
S I 1150.82	1150.8	0.3	...	Combined
Si II 1155.00	1154.9	0.3	...	Combined
Si II 1155.96	1155.8	0.3	...	Combined
S II 1163.20	1163.3	0.4	...	Combined
S II 1166.15, 1166.63	1166.4	1.7	...	Combined
C III 1174.60-1176.77	1175.2	2.5	...	Combined
Si II 1190.42	1190.5	0.6	...	Combined
Si II 1193.29	1193.4	0.4	...	Combined
Si II 1194.50	1194.5	0.5	...	Combined
N I 1200.22	1200.3	1.0	...	Combined
Si III 1206.50	1206.5	0.6	...	Combined
N V 1238.82	1238.8	0.4	...	Combined
N V 1242.80	1243.0	0.6	+0.2	1
	1242.8	0.6	0.0	2
	1243.3	0.6	+0.5	4
Si II 1250.58	1250.6	0.4	...	Combined
Si II 1253.81	1253.7	0.6	...	Combined
Si II 1259.92, 1260.42	1260.3	1.2	...	Combined
Si II 1264.74, 1265.00	1264.8	1.0	...	Combined
C I 1266.41	1266.2	0.1	-0.2	1,2,3,4,5
Al I 1271.77	1271.8	0.1	0.0	1,2,3,4,5
C I 1277.3, 1277.5	1277.4	1.0[a]	0.0	1,2,3,4,5
Si III 1298.89, 1298.95	1298.7	0.6[a]	-0.1	1
	1299.1	0.6[a]	+0.3	2
	1299.0	0.6[a]	+0.2	3,5
	1298.8	0.6[a]	0.0	4
O I 1302.17	1302.1	0.7[a]	-0.1	Combined
Si II 1304.37, O I 1304.86	1304.6	1.1[a]	...	Combined
O I 1306.03	1305.8	0.8	-0.2	Combined

Table 3—Continued

Line Identification	Line Center (Å)	Line Width (Å)	Line Shift (Å)	Orbit
Si II 1309.28	1309.2	0.7[a]	-0.1	Combined
N I 1316.04	1316.0	0.7[a]	0.0	Combined
N I 1319.67	1319.7	0.2	0.0	Combined
S III 1328.16-1328.81	1328.7	0.3	...	Combined
C I 1328.8	1329.1	0.3	...	Combined
C I 1329.60	1329.6	0.2	...	Combined
C II 1334.53, 1335.7	1334.7	2.4	-0.4	1
	1334.95	2.2	-0.15	2
	1335.2	2.4	+0.1	3,4,5
Si IV 1393.76	1393.3	1.0	-0.4	1
	1393.65	1.0	-0.1	2
	1393.85	1.0	+0.1	3,4,5
Si IV 1402.77	1402.35	1.0	-0.4	1
	1402.85	1.0	+0.1	3,4,5
N III 1410.08	1410.1	0.1	0.0	Combined
Si III 1417.24, Cu III 1418.43	1417.6	1.5	...	Combined
C III 1428.18	1428.2	0.3	...	Combined
Cu II 1442.14	1442.2	0.1	0.0	1,2,3,4,5
Co II 1443.84	1443.9	0.1	0.0	1,2,3,4,5
Co II 1456.27	1456.5	0.1	+0.2	1,2,3,4,5
C I 1463.34	1463.2	0.2	-0.1	Combined
Ni II 1467.26	1467.3	0.1	0.0	Combined
Ni II 1467.74	1467.9	0.1	0.1	Combined
N I 1492.63, 1492.82	1492.4	0.5	-0.3	1
	1492.8	0.5	+0.1	4
N I 1494.68	1494.7	0.2[a]	0.0	1
	1494.7	0.4[a]	0.0	4
Si II 1526.71	1526.5	1.0[a]	-0.2	1
	1526.8	1.0[a]	0.1	4

Table 3—Continued

Line Identification	Line Center (Å)	Line Width (Å)	Line Shift (Å)	Orbit
Si II 1533.43	1533.1	1.0^a	-0.3	1
	1533.4	1.0^a	0.0	4
C IV 1548.20	1547.6	1.0^a	-0.6	1
	1548.2	1.5^a	0.0	4
C IV 1550.78	1550.8	1.5^a	0.0	Combined
C I 1560.31-1561.44	1561.0	1.8^a	...	Combined
N II 1596.43	1596.7	0.1	+0.3	Combined
Fe II + C I 1608.4	1608.3	0.5	...	Combined
C I 1656.27-1658.12	1657.3	2.5	...	Combined
Al II 1670.79	1670.5	0.5^a	-0.3	1
	1670.8	0.5^a	0.0	4
Fe II 1673.46	1673.2	0.1	-0.3	1
	1673.5	0.1	0.0	4
S III 1713.11	1713.0	0.1	-0.1	Combined

[a]These lines also reveal a sharp absorption line at the bottom of the broad absorption line.

Table 4. 2004 July STIS temperature estimates

Exposure	Method	Log(g)	T_{wd} (1000K)	$V_{rot} \sin i$ (km/s)	Log R (cm)	Metallicity (solar)	χ^2_ν
Orbit 1	(a)	8.5	14.80	500	8.816	C=2.0 Si=0.2	1.113
Orbit 2	(a)	8.5	14.60	700	8.819	C=2.0 Si=0.2	1.005
Orbit 3	(a)	8.5	14.60	500	8.813	C=2.0 Si=0.2	0.932
Orbit 4	(a)	8.5	14.60	600	8.813	C=2.0 Si=0.2	0.900
Orbit 5	(a)	8.5	14.70	400	8.808	C=2.0 Si=0.2	1.408
Combined	(b)	8.5	15.50	300	8.760	0.5	0.900
Combined	(c)	8.0	14.44	267	8.836	0.7	1.174
Combined	(c)	8.5	15.41	260	8.760	0.7	1.127
Combined	(c)	9.0	16.45	245	8.686	0.7	1.083
Orbit 1	flux	8.5	15.40	-	-	-	-
Orbit 2-5	flux	8.5	15.00	-	-	-	-

Table 5. Accretional heating models for WZ Sge

Model number	M_{wd} $(M_\odot)$	$LogR_{wd}$ (cm)	Log(g) (cgs)	$T_{wd}^{i(1)}$ $(1,000K)$	$\dot{M}$ $(M_\odot/yr)$	ΔE (ergs)
1	0.8	8.845	8.34	12.5	4.0×10^{-08}	3.6×10^{39}
2	0.9	8.795	8.49	13.0	2.8×10^{-08}	2.9×10^{39}
3	1.0	8.745	8.64	13.5	2.0×10^{-08}	2.5×10^{39}
4	1.1	8.700	8.77	14.0	1.4×10^{-08}	2.4×10^{39}
5	1.2	8.600	9.00	14.5	9.0×10^{-09}	2.3×10^{39}
6	0.9	8.795	8.49	14.0	5.0×10^{-09}	7.0×10^{38}

[1]The initial quiescent temperature of the white dwarf at the beginning of each simulation.

Table 6. Boundary layer irradiation models for WZ Sge in quiescence

Model number	M_{wd} $(M_\odot)$	$LogR_{wd}$ (cm)	Log(g) (cgs)	$T_{wd}^{i(1)}$ $(1,000K)$	$\dot{M}$ $(M_\odot/yr)$	$T_{wd}^{(2)}$ $(1,000K)$
7	0.9	8.795	8.49	14.0	1.0×10^{-11}	15.5
8	0.9	8.795	8.49	14.0	2.0×10^{-11}	16.6
9	0.9	8.795	8.49	14.0	3.0×10^{-11}	17.5
10	0.9	8.795	8.49	14.0	5.0×10^{-11}	19.0
11	0.9	8.795	8.49	16.0	5.0×10^{-11}	20.0
12	0.9	8.795	8.49	16.0	1.0×10^{-10}	22.4

[1]The initial temperature of the white dwarf at the beginning of each simulation.

[2]The elevated temperature of the white dwarf due to boundary layer irradiation assuming a stellar rotation rate $\Omega_* = 0.2\Omega_K$.

Figures Caption

Figure 1: *HST/STIS* spectrum of WZ Sge obtained on 2004, July 11, almost 3 years after optical maximum, with suggested line identifications. The wavelength is given in Angström (Å) and the flux in erg cm^{-2}s^{-1}Å^{-1}. Note the scale is slightly different in each panel. In the last (bottom) panel, the stars denote regions where the echelles do not overlap and create gaps.

Figure 2: 2004 July 11 *HST/STIS* spectrum together with the 1989 August 26 *IUE* spectra (SWP36885). The flux level in 2004 (3 years after outburst) has still not yet reached the late quiescence (lower) flux level observed in 1989 with *IUE* (11 years after outburst).

Figure 3: July 2004 (combined) spectrum compared with the best-fitting log(g)=8.5 model computed in a manner similar to Long et al. (2004) - method (c). Top: Plots of the observed spectrum (black) and model spectra (red). Data that were excluded from the fitting (in the mapping technique) are plotted in green. The excluded regions are the double peak emissions from Lyα (H I around 1215 Å) and C IV (around 1550 Å) together with absorption lines not originating from the WD atmosphere (N V 1238.82 Å, 1242.80 Åand Si IV 1393.76 Å, 1402.77 Å). Bottom: Difference between the observed spectrum and the fitted spectrum (black); statistical error (two blue lines).

Figure 4: July 2004 (combined) spectrum compared with the best fitting log(g)=8.5 calculated in a manner similar to Godon et al. (2004) - method (b) (see Table 1 and text for details). The top panel shows the observed spectrum in solid black, the individual model components (WD + Gaussians) in black dotted lines and the sum of all components as a thick solid gray line. The bottom panel shows the residual, where the masked region (Lyα) has been omitted.

Figure 5: July 2004 (exposure # 2) spectrum compared with the best fitting log(g)=8.5 calculated in a manner similar to Godon et al. (2004) - method (a) (see Table 1 and text for details).

Figure 6: Modeling the heating and cooling of WZ Sge. The temperature (in Kelvin) of the white dwarf is drawn as a function of time (in days) since the start of the outburst (July 23, 2001). The solid line represents the compressional heating model with a 0.9 solar mass white dwarf (corresponding to Log(g)=8.5) with an initial temperature of 13,000K, accreting at a rate of $2.8 \times 10^{-8} M_{\odot}$/year for 52 days.

Figure 7: Same as Figure 6, but here the compressional heating model has a 0.9 solar mass white dwarf (corresponding to Log(g)=8.5) with an initial temperature of 14,000K, accreting at a rate of $5 \times 10^{-9} M_{\odot}$/year for 52 days. The compressional heating alone cannot

account for the observed elevated temperature of the WD.

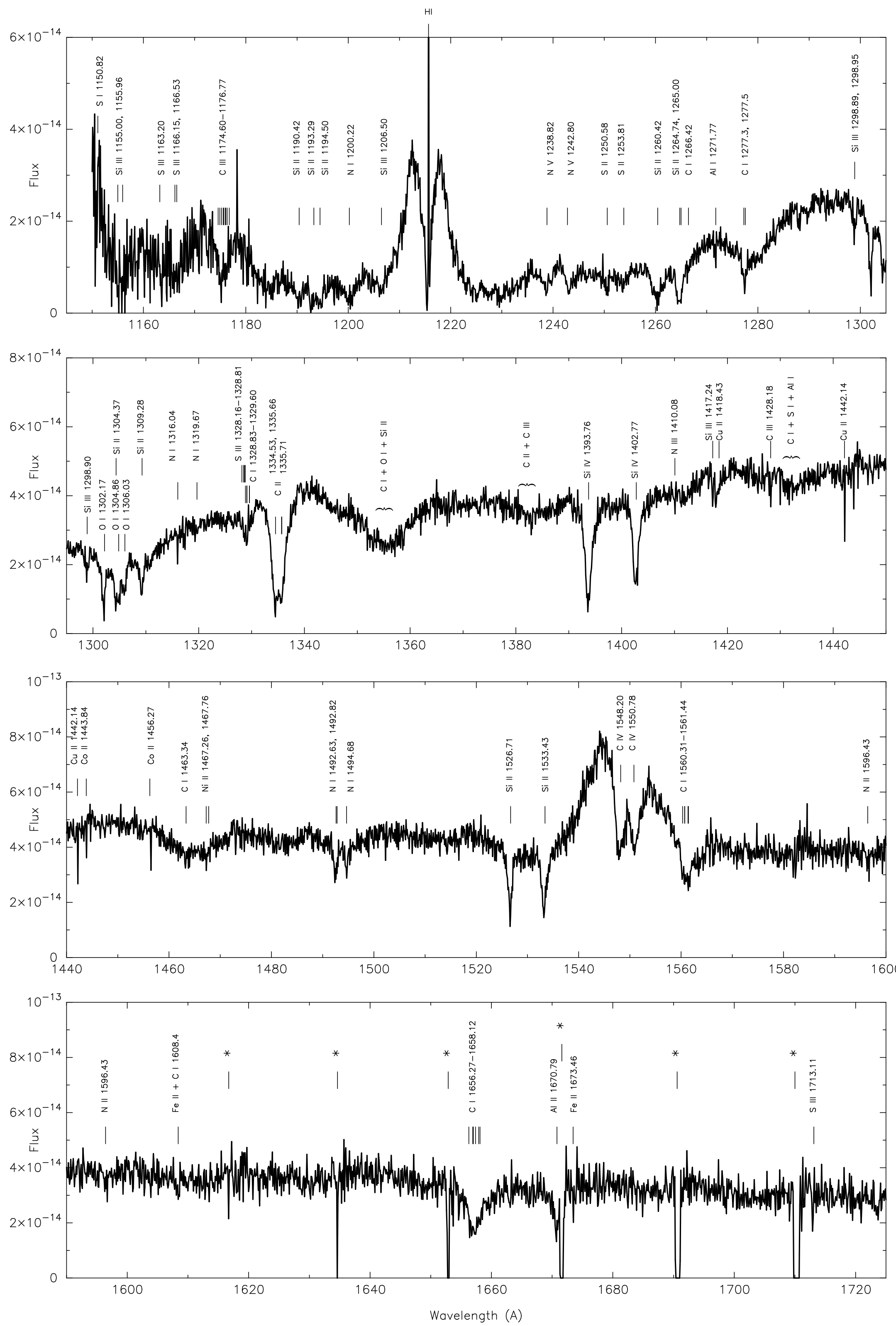
HI
S I 1150.82
Si III 1155.00, 1155.96
S III 1163.20
S III 1166.15, 1166.53
C III 1174.60–1176.77
Si II 1190.42
Si II 1193.29
Si II 1194.50
N I 1200.22
Si III 1206.50
N V 1238.82
N V 1242.80
S II 1250.58
S II 1253.81
Si II 1260.42
Si II 1264.74, 1265.00
C I 1266.42
Al I 1271.77
C I 1277.3, 1277.5
Si III 1298.89, 1298.95
Si III 1298.90
O I 1302.17
O I 1304.86
O I 1306.03
Si II 1304.37
Si II 1309.28
N I 1316.04
N I 1319.67
S III 1328.16–1328.81
C I 1328.83–1329.60
C II 1334.53, 1335.66
1335.71
C I + O I + Si II
C II + C III
Si IV 1393.76
Si IV 1402.77
N III 1410.08
Si III 1417.24
Cu II 1418.43
C III 1428.18
C I + S I + Al I
Cu II 1442.14
Cu II 1442.14
Co II 1443.84
Co II 1456.27
C I 1463.34
Ni II 1467.26, 1467.76
N I 1492.63, 1492.82
N I 1494.68
Si II 1526.71
Si II 1533.43
C IV 1548.20
C IV 1550.78
C I 1560.31–1561.44
N II 1596.43
N II 1596.43
Fe II + C I 1608.4
C I 1656.27–1658.12
Al II 1670.79
Fe II 1673.46
S III 1713.11
Flux
Wavelength (A)

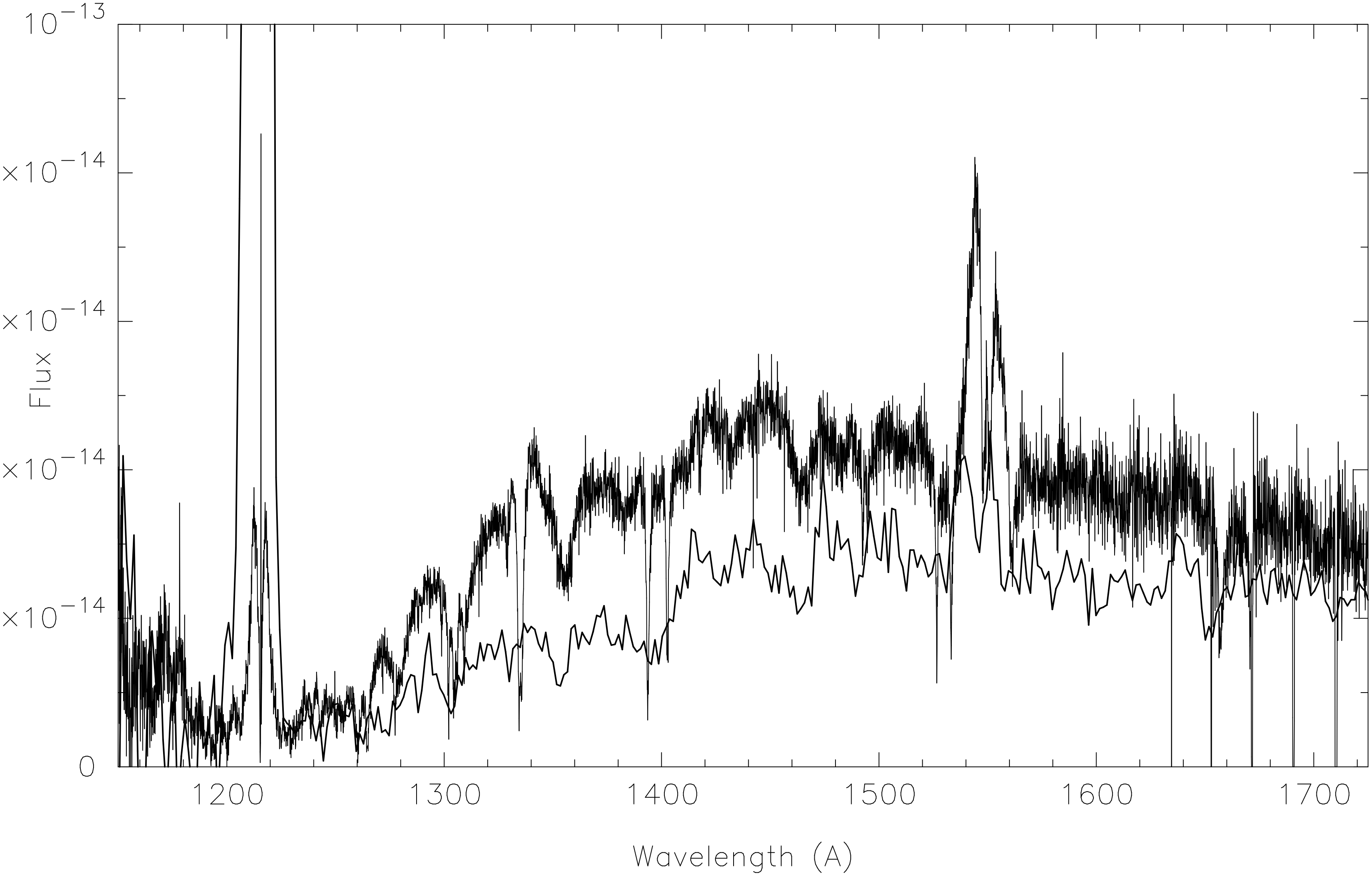

10^{-13}
8×10^{-14}
6×10^{-14}
4×10^{-14}
2×10^{-14}
0
Flux
1200
1300
1400
1500
1600
1700
Wavelength (A)

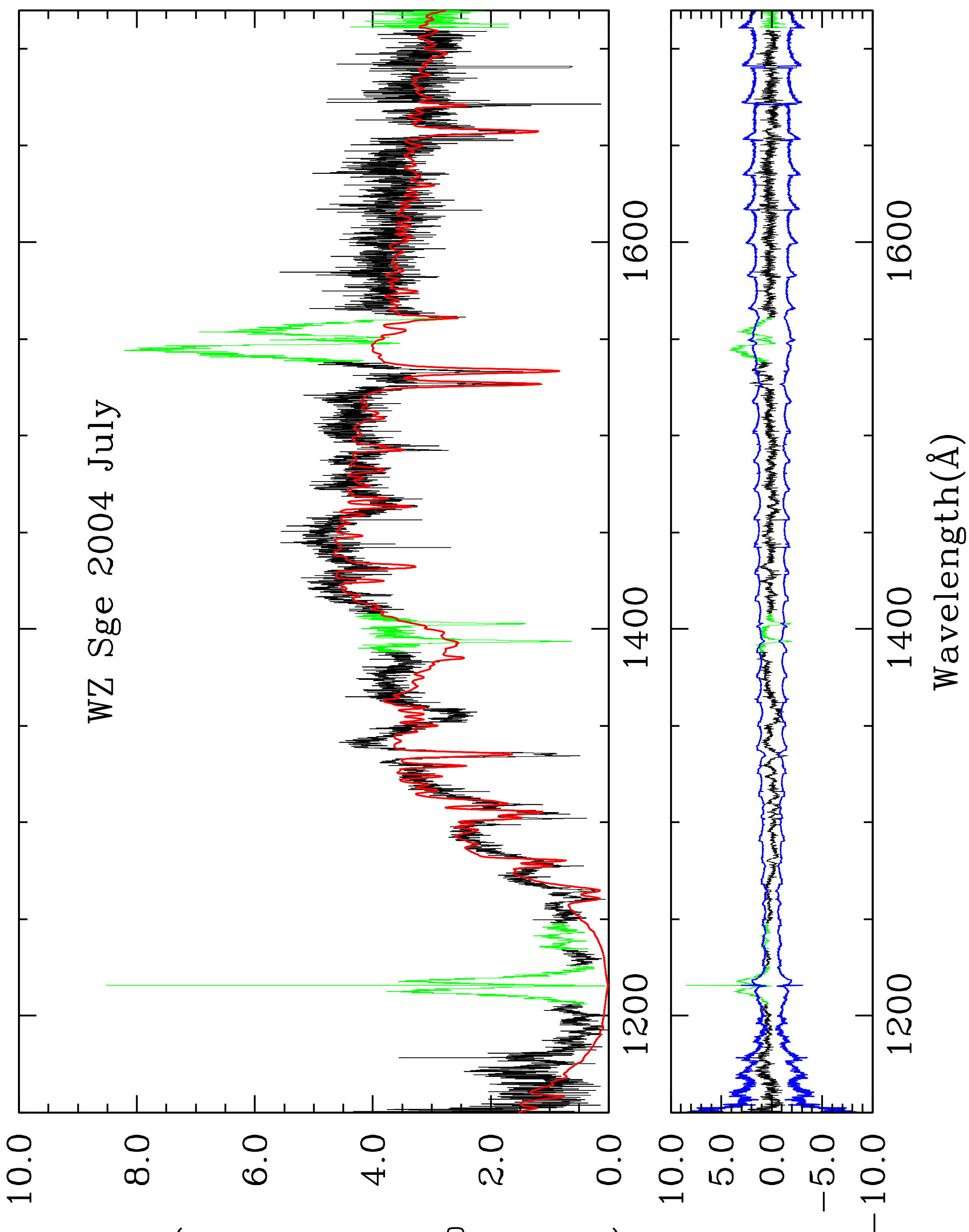
WZ Sge 2004 July
Flux (10-14 ergs cm-2 s-1 Å-1)
Wavelength(Å)
10.0
8.0
6.0
4.0
2.0
0.0
10.0
5.0
0.0
−5.0
−10.0
1200
1400
1600
1200
1400
1600

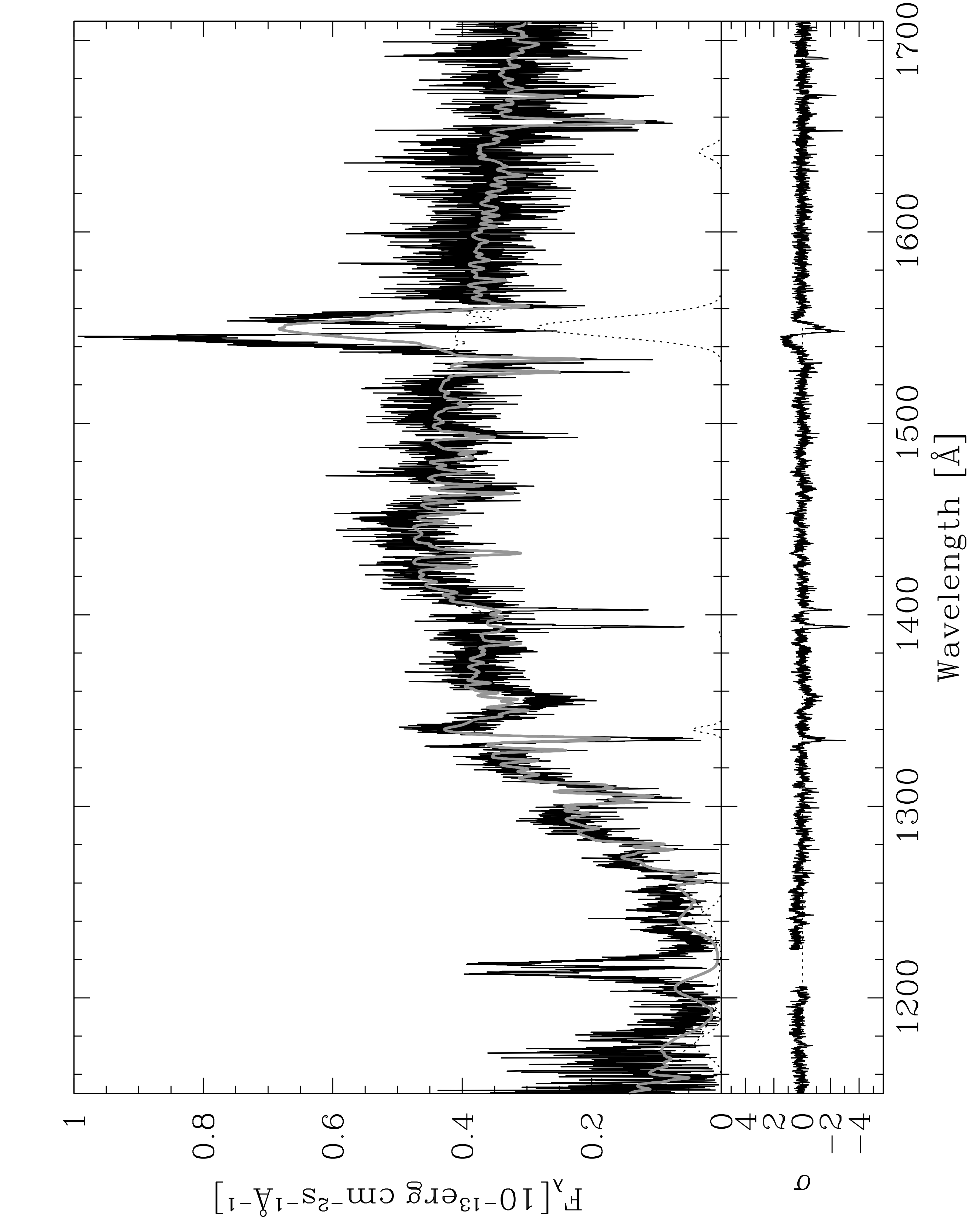
Wavelength [Å]
Fλ[10-13erg cm-2s-1Å-1]
σ

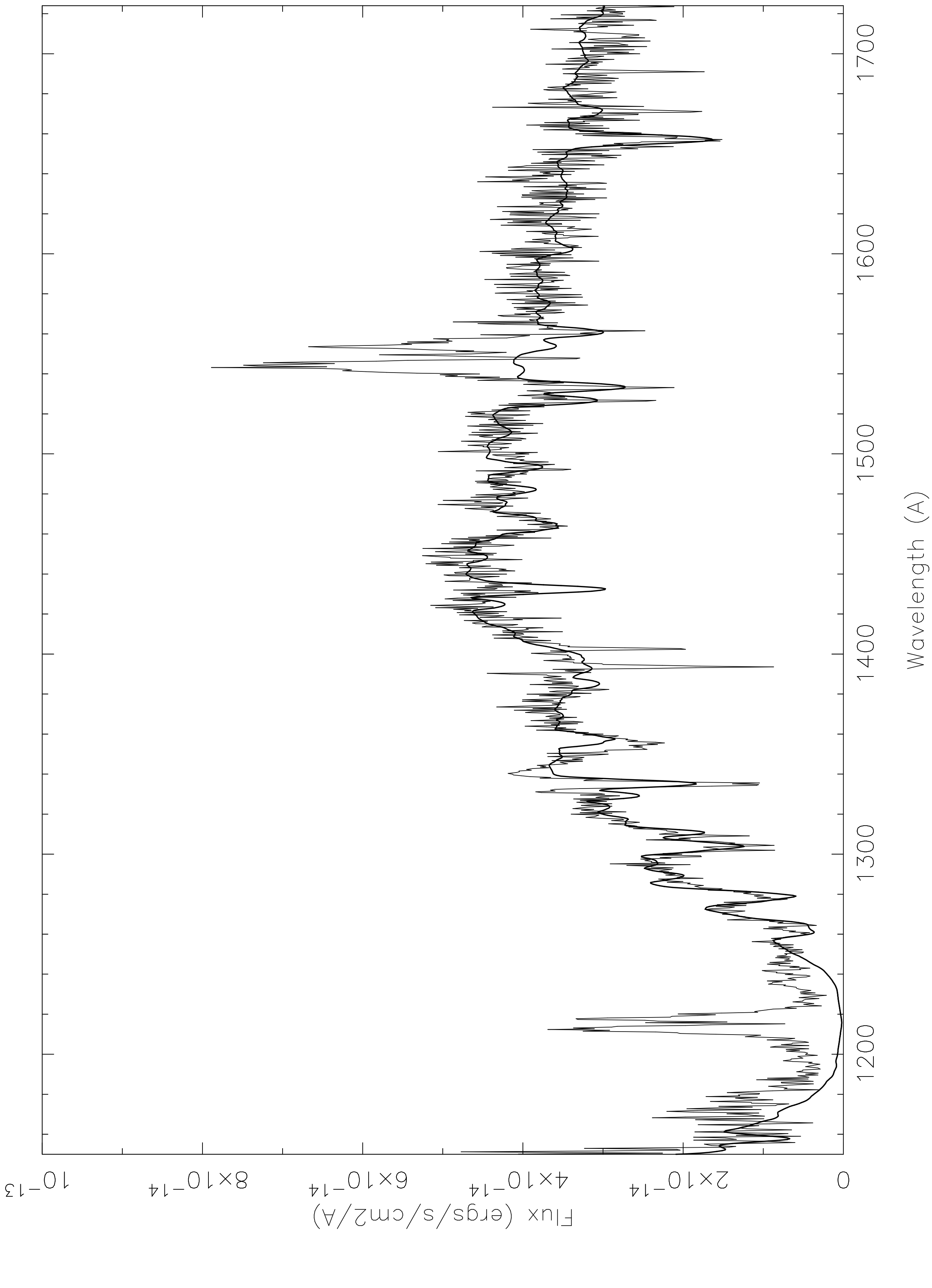

Wavelength (A)
1200
1300
1400
1500
1600
1700
Flux (ergs/s/cm2/A)
0
2×10⁻¹⁴
4×10⁻¹⁴
6×10⁻¹⁴
8×10⁻¹⁴
10⁻¹³

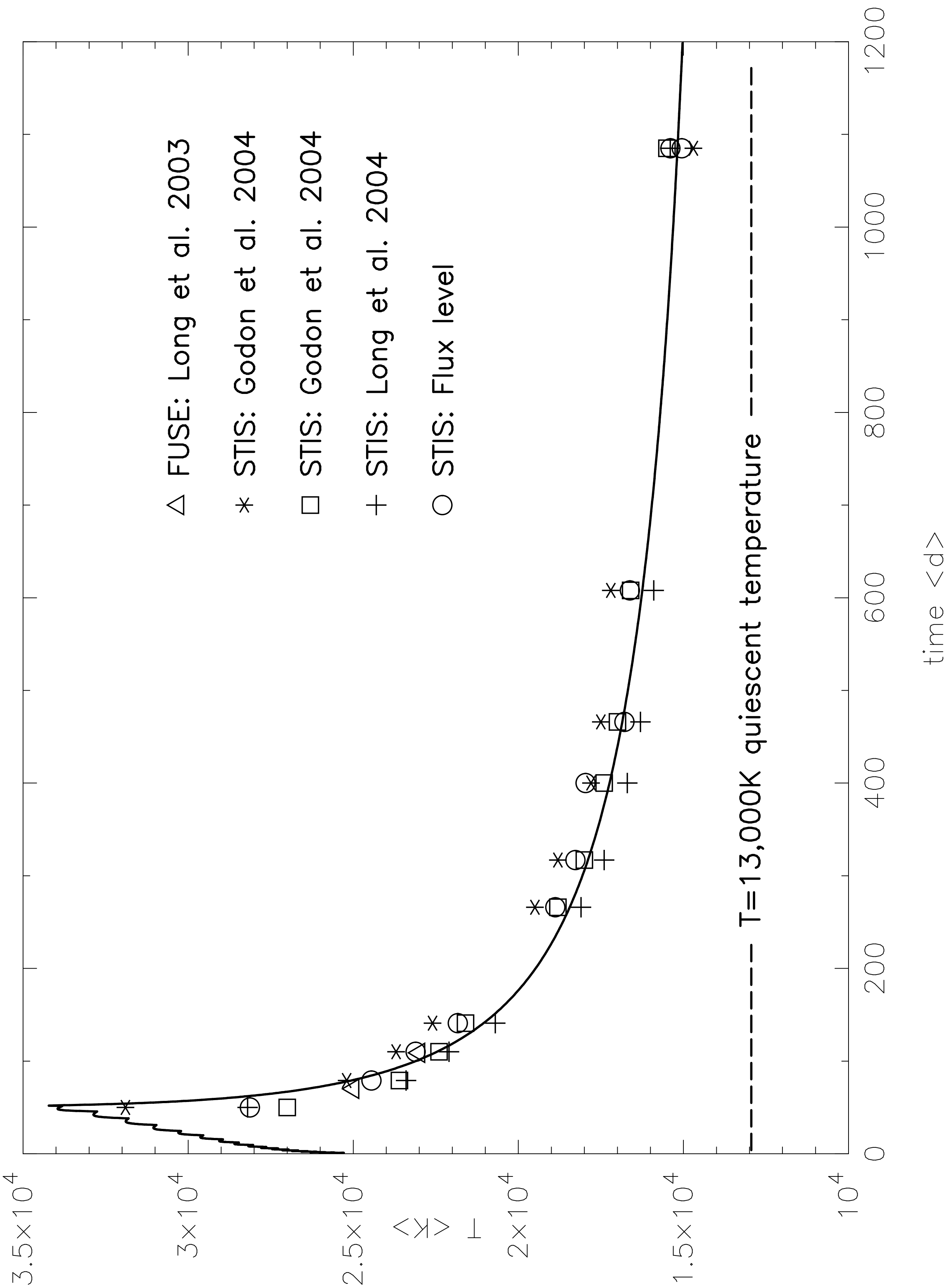

FUSE: Long et al. 2003
STIS: Godon et al. 2004
STIS: Godon et al. 2004
STIS: Long et al. 2004
STIS: Flux level
T=13,000K quiescent temperature
time <d>
T <K>
0
200
400
600
800
1000
1200
10^4
1.5×10^4
2×10^4
2.5×10^4
3×10^4
3.5×10^4

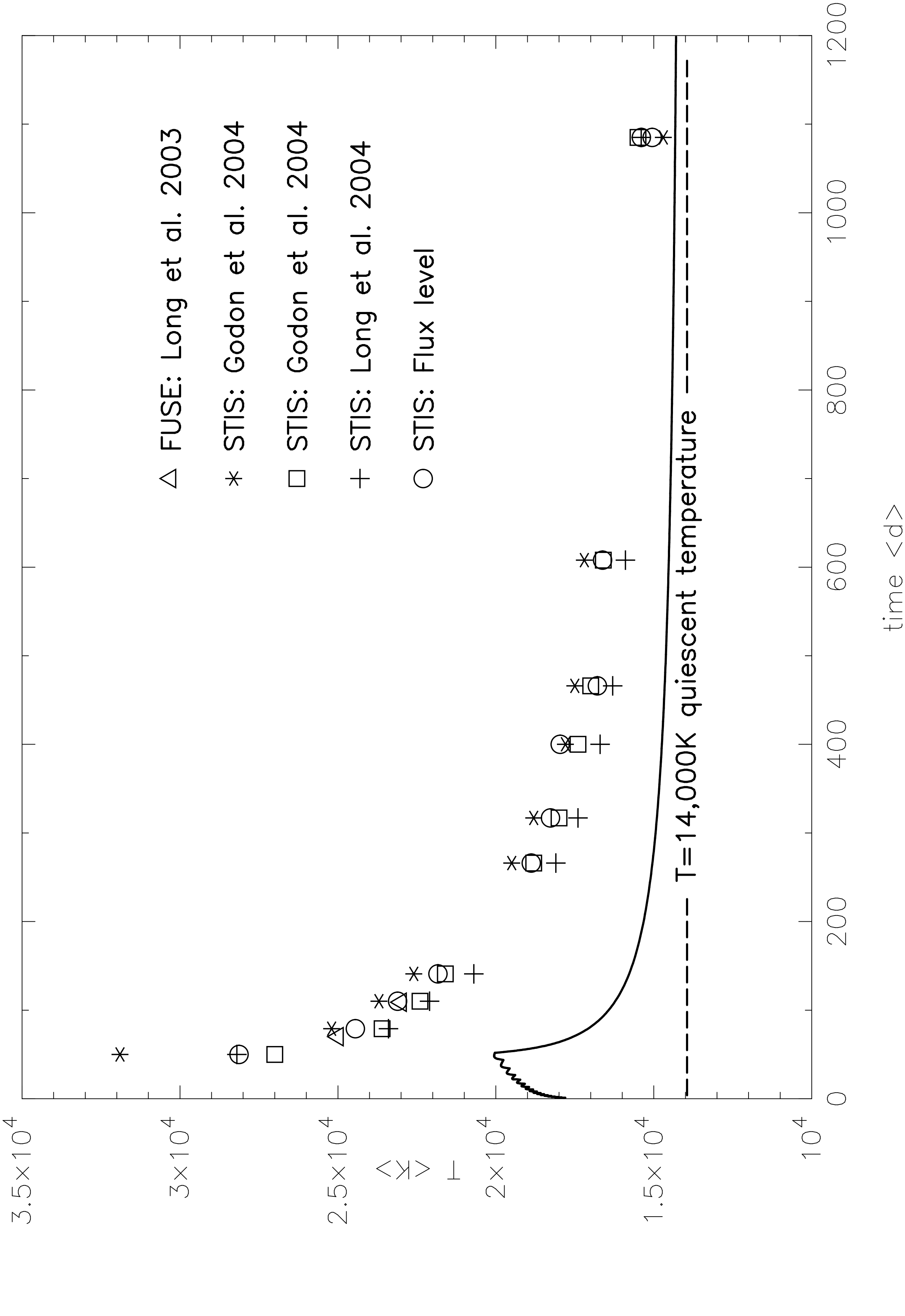

FUSE: Long et al. 2003
STIS: Godon et al. 2004
STIS: Godon et al. 2004
STIS: Long et al. 2004
STIS: Flux level
T=14,000K quiescent temperature
time <d>
T <K>
0
200
400
600
800
1000
1200
10^4
1.5×10^4
2×10^4
2.5×10^4
3×10^4
3.5×10^4